Spectroelectrochemical monitoring of contaminants during the electrochemical filtration process using free-standing carbon nanotube filters.

D. Ibañez,[a,] E. Gomez,[b] E. Valles,[b] A. Colina,[a] A. Heras.[a,*]*

a. Department of Chemistry, Universidad de Burgos, Pza. Misael Bañuelos s/n, 09001 Burgos, Spain.

b. Grup d'Electrodeposició de Capes Primes i Nanoestructures (GE-CPN). Dep. Ciència de Materials i Química Física and Institut de Nanociència i Nanotecnologia (IN2UB). Universitat de Barcelona, 08028 Barcelona, Spain.

* Corresponding author: dibanez@ubu.es; maheras@ubu.es.

ABSTRACT

Real-time process monitoring is still relatively scarce but is fundamental to provide *in-situ* information about different chemical and electrochemical processes. Particularly, electrochemical filtration has received growing attention in recent years due to the wide range of applications in which it can be successfully employed. Electrochemical removal is considered as an attractive methodology for the treatment of wastewater due to its efficiency in the removal of a huge number of contaminants. In this work, the development of a new device based on the use of UV-vis bare optical fibers in long optical pathway configuration allows us to monitor continuously the electrochemical degradation process during the filtration of different compounds. Spectroelectrochemistry additionally supplies quantitative information allowing us to calculate the efficiency of the electrochemical filtration process. The material selected to fabricate the electrochemical filter was single-walled carbon nanotubes that display not only high physical and chemical stability, but also high electrical conductivity. Therefore, the combination of electrochemical degradation methods, free-standing single-walled carbon nanotube filters and operando spectroelectrochemical techniques makes this outstanding device very interesting in the study of different molecules. As proof of concept, three different systems have been studied to validate the cell and demonstrate the good performance of the spectroelectrochemical device: *o*-tolidine (reference system), indigo carmine (organic dye), and 4-nitrophenol (hazardous pollutant).

KEYWORDS

Real-time monitoring; electrochemical filters; UV-vis spectroelectrochemistry; single-walled carbon nanotubes; pollutants.

1. Introduction

Electrochemical detection and treatment of wastewater is an overwhelming subject that has received growing attention from the scientific community in a wide variety of fields, such as chemical, petrochemical, pharmaceutical, textile, tannery, food industry, agronomic, landfill leachate and urban wastewater [1–15]. Electrochemical filtration enables the removal of contaminants by adsorptive filtration, as well as electrochemical degradation of different molecules under a suitable applied potential. The versatility shown by these methods makes them very useful in the degradation of a wide range of contaminants. The development of new devices for i*n-situ* real-time monitoring of electrochemical filtration processes allows to study and control the different kind of phenomena involved for a huge variety of systems [16–20]. *In-situ* spectroelectrochemical monitoring provides dynamic spectroscopic and electrochemical information at the same time that the redox reaction takes place. This is the main advantage respect to *ex-situ* methods that require taking one or more samples and analyzing it or them using external instruments. The implementation of real-time monitoring devices in agreement with the specific demands of the process provides direct information about all of these processes. These new devices will supply unique and outstanding possibilities very useful for good process control.

Although the interesting properties of carbon nanotube (CNT) filters are well-known [21–28], the simultaneous combination of this material with spectroelectrochemical techniques are notably absent in the literature for evaluation of filtration processes. Spectroelectrochemistry is a multiresponse technique that provides simultaneous electrochemical and spectroscopic information in a unique experiment. It shows the advantages of both techniques and offers very unique possibilities in the study of a huge variety of chemical systems [29–32].

Spectroelectrochemical measurements has allowed the monitoring of a wide range of systems, fundamental aspects as reaction mechanisms, or quantitative analysis [33–38].

The main objective of this work is the in-situ monitoring of the electrochemical treatment of different compounds using a new UV-vis absorption spectroelectrochemical filtration device, showing the capabilities and advantages of this novel setup in the study of the behavior of the designed electrochemical filter. We have analyzed three electrochemical systems to illustrate, in a general way, the good performance of this UV-vis absorption spectroelectrochemical filtration device. Firstly, *o*-tolidine (*o*-tol) has been chosen as reference system to validate the operation of the new spectroelectrochemical filtration setup. *O*-tol is a well-known reference system for UV-vis absorption spectroelectrochemistry that exhibits a fast two electron transfer, and is widely used because it has a large molar absorption coefficient in water [39,40]. The second system studied was indigo carmine (IC), an organic dye employed in different fields not only as a dye in the pharmaceutical and food industry but also as redox indicator and mediator in biological systems [41,42]. Finally, the new spectroelectrochemical filtration device was employed to study the electrochemical reduction of 4-nitrophenol (4-NP). For the last decades, 4-nitrophenol has become one the most used compounds in the fabrication of drugs, pesticides, or leather [43–45]. However, 4-NP is a hazardous pollutant for humans, plants and animals, and in this way, it is important to eliminate this compound from the wastewater, atmosphere and ground because is one of the nitrophenols in the U. S. Environmental Protection Agency List of Priority Pollutants [46,47]. Furthermore, not only the use of 4-NP has increased in the industry during the last years, but also in other areas such as, for example, in agriculture, medical applications and domestic activities [48–50]. Although different methods can be followed to get rid of 4-NP of the industrial wastewater, our interest is focused on the electrochemical removal due to the

simplicity to automatize this methodology, its high level of efficiency and its great compatibility with the environment [51,52]. The combination of electrochemical and UV-vis absorption spectroscopy techniques has allowed monitoring the degradation of 4-NP from an aqueous solution.

2. Materials and methods

2.1. Reagents and materials

Ammonium hexafluorophosphate (NH_4PF_6, Fluka), *o*-tolidine (*o*-tol, Sigma-Aldrich), acetic acid (HAc, VWR), perchloric acid ($HClO_4$, 60%, Panreac), indigo carmine (IC, Acros Organics), sulfuric acid (H_2SO_4, 95-97%, Merck), 4-nitrophenol (4-NP, Sigma-Aldrich) and sodium sulfate (Na_2SO_4, Merck) were of analytical grade. Aqueous solutions were freshly prepared, or stored at 4 ºC, using ultrapure water (18.2 MΩ cm resistivity at 25 °C, Milli-Q Direct 8, Millipore).

Single-walled carbon nanotubes (SWCNTs, Sigma-Aldrich), 1,2-dichloroethane (DCE, 99.8% for HPLC, Acros Organics), acetone (VWR), nitrocellulose membrane (filter pore size 0.45 μm, Millipore), poly(ethylene terephthalate) (PET, 175 mm thick, HiFi Industrial Film), conductive silver paint (Electrolube) for ohmic contacts, and a high temp masking tape (Kapton) were used to fabricate the free-standing single-walled carbon nanotube (FS-SWCNT) filters.

2.2. Instrumentation

All electrochemical measurements were carried out at room temperature using a potentiostat/galvanostat AUTOLAB PGSTAT 302N electrochemical system. A standard three-electrode cell was used in all experiments, consisting of a FS-SWCNT electrode as working

electrode, a Pt wire as counter electrode and a homemade Ag/AgCl/KCl (3 M) as reference electrode.

UV-vis absorption spectroelectrochemistry measurements in parallel configuration (the light beam passes parallel and close to the electrode surface) [53] were performed using a QE65000 spectrometer (Ocean Optics). UV-vis spectrometer was properly synchronized with the potentiostat. The light beam, supplied by a light source (Halogen HL-2000, Avantes), was conducted to the spectroelectrochemical cell by a 100 μm bare optical fiber (Ocean Optics), and collected from the spectroelectrochemical cell to the spectrometer by a 100 μm bare optical fiber (Ocean Optics).

Raman spectra were obtained using a Confocal Raman Voyage (BWTEK). A 20× objective was used, with an excitation line at 532 nm and a power of 5 mW. Raman spectra were collected by a CCD array, with a spectral resolution of 3.8 cm^{-1}.

Morphology was studied using a scanning electron microscope Field Emission JSM-7100F Analytical Microscopy.

Atomic-force microscopy (AFM) measurements were carried out using a Alpha300R - Alpha300A AFM WITec.

2.3. Fabrication of free-standing carbon nanotube filters

The methodology employed in the preparation of FS-SWCNT filters is based on previous works [37,54,55]. Briefly, it consists of seven consecutive steps: (1) Preparation of a homogeneous dispersion of SWCNTs in DCE (5 mg/L). Homogeneous dispersion is achieved using a CY-500 tip-sonicator (Optic ivymen System), applying a power of 250 W for 10 min and reducing the power to 100 W for another 5 min. (2) Filtration of 3 mL of the SWCNT dispersion

under vacuum using a nitrocellulose filter. (3) Transference of the SWCNT film to a poly(ethylene terephthalate) (PET) sheet with a hole of 2 mm diameter applying a gentle pressure around the edges of the nitrocellulose filter to improve adhesion of the SWCNT film to the PET. (4) Dissolution of the nitrocellulose filter by slow addition of acetone and rinsing of the SWCNT film with acetone for 15 min to ensure the complete removal of the filter. (5) Drying at room temperature of the SWCNT film. (6) An ohmic contact is made using a conductive silver paint that is dried in an oven at 75 °C for 30 min. (7) Isolation of the the ohmic contact with a high temperature masking tape.

2.4. Characterization of the free-standing SWCNT electrodes.

Optimization of FS-SWCNT films was performed in a previous work [53]. The electrodes prepared by filtering 3 mL of the SWCNT dispersion display the best features for spectroelectrochemical purposes. Characterization of FS-SWCNT electrodes was performed by Raman spectroscopy. Fig. S1 shows the characteristic Raman spectrum of the SWCNTs, in which mainly four bands are observed: the radial breathing mode (150-250 cm^{-1}, RBM), the disorder induced mode (1250-1450 cm^{-1}, D), the tangential displacement mode (1550-1600 cm^{-1}, G) and the high frequency two phonon mode (2500-2800 cm^{-1}, G') [47–52].

SEM image (Fig. S2) shows that FS-SWCNT film is completely uniform. As was establish in a previous work [53], the flexibility of this kind of films is an important property, FS-SWCNT electrodes remain intact even when the PET sheet is completely bent. Thickness of the 3 mL film was determined by AFM, obtaining a value of 570 ± 30 nm. Optical transparency of the film was evaluated by measuring the transmittance at 550 nm, obtaining a transmittance value of 18 ± 2 %.

2.5. Electrochemical hydrophilization of free-standing carbon nanotube films

Although different methods can be followed to obtain hydrophilic carbon nanostructures [56,57] our interest is focused on the electrochemical route because this procedure is cleaner and faster [58–60]. Typically, the oxidation of carbon nanotubes introduces functional groups (hydroxyl, carbonyl, carboxyl or epoxide groups) into the molecular structure, providing hydrophilic properties to carbon structures [61]. The electrochemical functionalization was performed in 0.1 M NH_4PF_6 by chronoamperometry applying 0.00 V, 10 s; +1.20 V, 20 s; 0.00 V, 10 s; +1.40 V, 20 s; 0.00 V, 10 s; +1.60 V, 20 s; 0.00 V, 10 s and +1.80 V, 20 s (Fig. 1a). Using this multipulse-potential sequence, SWCNTs are gradually oxidized until its pristine hydrophobic character turns to a hydrophilic one. Hydrophobic/hydrophilic character of FS-SWCNT filters was demonstrated before and after the electrochemical functionalization. As can be observed in Fig. 1b, FS-SWCNT films show hydrophobic properties, and the solution cannot pass through the filter and drops are not observed on the bottom side of the filter. On the other hand, after the electrochemical functionalization (Fig. 1c) the solution passes from the upper side to the bottom side of the FS-SWCNT filter after 10 seconds approximately. Fig. 1 demonstrates that the electrochemical functionalization is a suitable route to obtain hydrophilic SWCNTs following an easy, clean, quick, cheap, and reproducible methodology. Moreover, instrumentation required is not complicated, which makes this method a very useful alternative to the chemical route.

2.6. Spectroelectrochemical setup

The setup proposed in this work (Fig. 2 and Fig. S3 in Supporting Information) involves a FS-SWCNT working electrode (WE), a homemade Ag/AgCl/KCl 3M reference electrode (RE) and a Pt wire as counter electrode (CE). A cylindrical vessel to contain the initial solution is fixed on the upper side of the WE. Electrochemical oxidation/reduction reaction, depending on the system studied, was followed by UV-vis absorption spectroelectrochemistry. For a better monitoring of the processes occurring during the electrochemical reaction, spectroelectrochemical measurements were carried out in parallel arrangement. For this purpose, two bare optical fibers are aligned opposite one another and fixed on the bottom side of the FS-SWCNT membrane to record the spectral changes. Therefore, one 100 µm bare optical fiber (F_1) leads the light beam from the light source and is accurately aligned with a second 100 µm bare optical fiber (F_2) that collects the transmitted light beam to the spectrometer. The light beam in parallel configuration passes parallel and close to the electrode surface, sampling only the first 100 µm of solution adjacent to the FS-SWCNT film. The two 100 µm bare optical fibers are properly fixed on the bottom side of the FS-SWCNT filter at a known distance. Optical pathway lengths were set between 0.04-0.10 cm depending on the experiment.

Furthermore, spectroelectrochemical information not only provides qualitative information but also quantitative information that can be used to calculate the efficiency of the degradation process using FS-SWCNT electrochemical filters. In all experiments, the spectrum of the initial solution with the electroactive compound was taken as reference spectrum before starting the cyclic voltammetry. Theoretical maximum absorbance value (when 100% of the initial compound is converted into the final product) is calculated according to the Lambert-Beer's law:

$$A_{theoretical} = \varepsilon \cdot b \cdot C \qquad \text{(eq. 1)}$$

where ε is the molar absorption coefficient, b is the optical pathway length (determined by the distance between the two bare optical fibers), and C is the electroactive compound concentration. Experimental maximum absorbance value is extracted from the UV-vis spectra and the efficiency (r) of this FS-SWCNT filter is calculated as:

$$r = \frac{A_{experimental}}{A_{theorethical}} \times 100 \qquad \text{(eq. 2)}$$

However, the molar absorption coefficient is not always known and the efficiency of the electrochemical process cannot be calculated. UV-vis absorption spectroelectrochemistry allows us to calculate this value at any wavelength of the UV-vis spectral region using eq. 3 (see details in Section S1 of the Supporting Information) [53]:

$$A_N = (\varepsilon_B - \varepsilon_A)\frac{10^3}{n \cdot F \cdot S}Q = \Delta\varepsilon\frac{10^3}{n \cdot F \cdot S}Q \qquad \text{(eq. 3)}$$

where A_N is the absorbance in normal configuration (the light passes through the solution perpendicularly to the electrode surface) [53], ε_A and ε_B are the molar absorption coefficients of initial and final species, respectively, $\Delta\varepsilon$ is the difference between these two molar absorption coefficients, n is the number of electrons, F is Faraday's constant, S is the area of the electrode and Q is the total electric charge passed during the experiment. As can be observed, in this case UV-vis absorption measurements in normal configuration are required instead of those in parallel configuration [53]. Absorbance changes in spectroelectrochemistry experiments are related to the concentration changes of redox-active compounds in the diffusion layer and parallel arrangement only provides information of the first micrometers of solution adjacent to the electrode.

3. Results and discussion

3.1. Validation of the electrochemical filter with o-tolidine

The experimental setup for spectroelectrochemical measurements (Fig. 2) was validated using *o*-tol because it is a well-known molecule commonly used in UV-vis absorption spectroelectrochemistry. In order to select the potential that will be applied to study the oxidation of *o*-tol to *o*-tolidinium cation by UV-vis spectroelectrochemistry, a previous cyclic voltammetry was performed. Fig. S4 in Supporting Information displays the cyclic voltammogram obtained scanning the potential from +0.40 V to +0.80 V and back to +0.40 V at 0.01 V s^{-1} in 1 × 10^{-4} M *o*-tol, 0.5 M HAc and 1 M $HClO_4$ solution using a SWCNT working electrode. Voltammetric experiment (Fig. S4 in Supporting Information) shows an anodic peak at +0.63 V related to the electrogeneration of *o*-tolidinium cation in the forward scan, and a reversible cathodic peak at +0.58 V that is related to the reduction of this cation to *o*-tol in the backward scan [39]. According to the cyclic voltammogram, the potential selected to study the oxidation of *o*-tol using the electrochemical filter was +0.80 V. Although this potential is more positive than the anodic peak observed in the cyclic voltammogram (+0.63 V), it allow us to be completely sure that *o*-tol will be oxidized to *o*-tolidinium cation.

Spectroelectrochemical oxidation of *o*-tol was performed by chronoamperometry in 1 × 10^{-4} M *o*-tol, 0.5 M HAc and 1 M $HClO_4$ solution using a FS-SWCNT filter. Video S1 in Supporting Information shows the spectroelectrochemical performance of FS-SWCNT electrochemical filters with the experimental setup shown in Fig. 2. Video S1 in Supporting Information evidences the oxidation of *o*-tol to *o*-tolidinium cation by changes in the colorless starting solution to a yellowish one at the end of the experiment. In order to quantify this oxidation process, UV-vis spectroelectrochemical measurements in parallel configuration were performed.

Electrochemical experiment consisted of two steps, the first one in which no potential (open circuit) was applied during 50 s and the second one, in which a chronoamperometry was carried out at +0.80 V for 150 s. Fig. 3a displays the UV-vis spectra recorded during the electrochemical oxidation of *o*-tol to *o*-tolidinium cation. The spectrum of the initial solution (*o*-tol) was taken as reference for the UV-vis absorption spectra. As can be observed, an absorption band related to *o*-tolidinium cation emerges at 438 nm. Fig. 3b shows the comparison between the electrochemical response (brown line) and evolution of UV-vis absorption band at 438 nm (blue line) along the chronoamperometric experiment. Both signals display several periodic peaks that correspond to the falling of each drop generated on the bottom side of the filter while the solution fluxes through the FS-SWCNT. Chronoabsorptogram at 438 nm (blue line) shows that the absorbance does not change during approximately the first 50 s when no potential was applied. However, the absorbance shows a sharp increase when the potential of +0.80 V was applied. Absorbance value increases as the solution passes through the filter, the *o*-tolidinium cation is electrogenerated and the drop is formed, while it decreases when the drops fall down. Conversely, the current intensity in the electrochemical signal (brown line) decreases when the solution with the *o*-tolidinium cation passes through the filter and a new drop is generated in the bottom side of the FS-SWCNT, whereas it increases abruptly when each droplet falls. Hence, electrochemical and spectroscopic signals are completely correlated and thus, the spectroelectrochemical FS-SWCNT filtration device was validated, demonstrating that this kind of filters is useful to remove different species by electrochemical processes.

Spectroelectrochemical information allows us to calculate the efficiency of the oxidation *o*-tol using FS-SWCNT electrochemical filters. According to the Lambert-Beer's law (eq. 1) and being $\varepsilon_{o\text{-tolidinium cation}} = 60670$ L mol^{-1} cm^{-1} at 438 nm [39,40], $b = 0.099$ cm, and $C = 1 \times 10^{-4}$ M,

the $A_{theoretical}$ value was 0.601 a.u. (eq. 1). On the other hand, the experimental maximum value of absorbance observed in Fig. 3b is 0.558 a.u., so the efficiency of the electrochemical process (eq. 2) was r = 93 %, demonstrating the good performance of the spectroelectrochemical device.

3.2. Removal of indigo carmine

This molecule is a dye commonly used in the pharmaceutical and food industry. An aqueous solution of 1×10^{-4} M IC in acid media (1 M H_2SO_4) avoids the formation of dimers in solution and ensures that the dimerization equilibrium is shifted towards the monomeric form [62]. Prior to study its spectroelectrochemical behavior using FS-SWCNT filters, an electrochemical study was performed by cyclic voltammetry (Fig. S5 in Supporting Information) in 1×10^{-4} M IC and 1 M H_2SO_4 solution, scanning the potential from +0.20 V to -0.10 V and backwards to +0.20 V at 0.01 V s^{-1} using a SWCNT electrode. As can be noticed in the cyclic voltammogram, a cathodic peak at +0.03 V related to the electrogeneration of leuco-IC is observed in the forward scan [63]. On the other hand, in the anodic scan a peak at +0.07 V related to the oxidation of leuco-IC to the initial IC is observed. According to the cyclic voltammogram, the potential selected to study the reduction of IC by UV-vis absorption spectroelectrochemistry was -0.10 V.

Removal of IC was performed by chronoamperometry in 1×10^{-4} M IC in 1 M H_2SO_4 solution using a FS-SWCNT filter. As in the previous case, during the first 50 s no potential was applied. After this time, chronoamperometry was carried out at -0.10 V for 100 s. Fig. 4a displays the UV-vis spectra recorded during the electrochemical reduction of IC to leuco-IC. The spectrum of the initial solution was taken as reference for the UV-vis absorption spectra. As can be noticed, two absorption bands emerge in the UV-vis spectra at 372 and 617 nm [64]. Fig. 4b shows the comparison between the electrochemical response (brown line) and evolution of UV-

vis absorption band at 617 nm (blue line). As occurs with *o*-tol (Fig. 3b), both signals show different periodic peaks associated with generation and falling down of a droplet with the reduced form of IC in the bottom side of the FS-SWCNT filter, process cyclically repeated along the chronoamperometric experiment. Although during approximately the first 50 s absorbance does not change, it decreases when -0.10 V is applied because IC is consumed and leuco-IC is generated. Absorbance value slightly increases as the solution passes through the filter and the droplet is formed, while the fall of the drops produces small and periodic decrease of absorbance at 617 nm. It should be noted, that absorbance takes negative values because the spectrum of the initial solution was taken as reference for the UV-vis absorption spectra. IC exhibits a band around 617 nm (A = 0 a.u. at t = 0 s), that decreases when IC is reduced to leuco-IC (A = -0.081 a.u. at t > 50 s). Evolution of absorbance at 372 nm shows the same behavior than band at 617 nm but with opposite sign, because is related to the generation of leuco-IC. The electrochemical signal (brown line) shows that the current decreases when leuco-IC passes through the filter and it increases when each droplet falls. As in the *o*-tol experiments, electrochemical and spectroscopic signals totally agree, showing the utility of the spectroelectrochemical FS-SWCNT filtration setup for monitoring the degradation of dye in pharmaceutical and food industry.

In order to check the suitable performance of the spectroelectrochemical device with this extremely colored dye, the efficiency of the reduction and filtration process was evaluated, selecting the absorbance values at 617 nm. At this wavelength the two compounds, IC and leuco-IC absorb UV-vis radiation. The molar absorption coefficient of leuco-IC at 617 nm was assessed because this coefficient cannot be found in literature. With this objective, linear regressions of absorbance in normal configuration (A_N) *vs* the electric charge involved in the redox process (Q) for the experiments at different scan rates were performed (eq. 3) [53]. From

the slopes of the linear regressions, and being n = 2, F = 96485 C mol^{-1}, and S = 0.056 cm^2, the difference of the molar absorption coefficients of leuco-IC and IC ($\Delta\varepsilon$) can be obtained at any wavelength of the UV-vis spectral region using eq. 3. The experimental Δε value obtained from the slopes was 10181 M^{-1} cm^{-1}. On the other side, the molar absorption coefficient of IC at 617 nm was obtained by spectrophotometric calibration, ε_{IC} = 15190 M^{-1} cm^{-1}. With these two values, $\Delta\varepsilon$ and ε_{IC}, the molar absorption coefficient of leuco-IC at 617 nm was calculated, $\varepsilon_{leuco\text{-}IC}$ = 5009 M^{-1} cm^{-1}. Once the two molar absorption coefficients for IC and leuco-IC are estimated, the efficiency of the electrochemical degradation of IC is calculated. According to the Lambert-Beer's law (eq. 1), being $\Delta\varepsilon$ = 10181 L mol^{-1} cm^{-1} [39], b = 0.085 cm and $C = 1 \times 10^{-4}$ M, the $A_{theoretical}$ was 0.086 a.u., while the experimental maximum value at 617 nm observed in Fig. 4 is 0.081 a.u. The efficiency of the electrochemical process was 94 %, demonstrating the good performance of the spectroelectrochemical device to quantify the electrochemical degradation process of dyes.

3.3. Degradation of 4-nitrophenol

The interest in this compound lies in its toxicity and its wide presence in industrial waste. Electrochemical reduction offers an easy possibility of degradation from 4-NP to 4-aminophenol (4-AP) in wastewater. In order to select the reduction potential that will be applied to study the reduction of 4-NP to 4-AP, a previous cyclic voltammetry was performed scanning the potential from 0.00 V to -0.60 V and back to 0.00 V at 0.01 V s^{-1} in 5×10^{-4} M 4-NP and 0.05 M Na_2SO_4 solution using a SWCNT electrode (Fig. S6 in Supporting Information According to the cyclic voltammogram, reduction of 4-NP to 4-AP is an irreversible process because oxidative peaks are not observed in the backward scan, showing only a cathodic peak at -0.43 V related to the 4-AP

electrogeneration in the forward scan. The potential selected was -0.60 V because this potential accomplishes well the reduction requirement.

Spectroelectrochemical reduction of 4-NP was carried out by chronoamperometry in 5×10^{-4} M 4-NP and 0.05 M Na_2SO_4 solution using a FS-SWCNT filter. A chronoamperometry was performed at -0.60 V for 200 s. Fig. 5a shows the UV-vis spectra recorded during the electrochemical reduction of 4-NP to 4-AP. The spectrum of the initial solution (4-NP) was taken as reference for the UV-vis absorption spectra. UV-vis spectra shows two absorption bands that emerge at 332 and 405 nm related to the consumption and generation of 4-NP and 4-AP, respectively. Fig. 5b shows the comparison between the electrochemical response (brown line) and evolution of UV-vis band at 405 nm (blue line). A similar behavior is observed in the two signals recorded during the chronoamperometric experiment, absorbance at 405 nm and the intensity current increased along the 200 s the potential of -0.60 V is applied. As in the experiments described above for the other two chemical systems, periodic peaks are observed in the two signals related to the falling down of each drop generated in the bottom side of the filter after passing the flux through it: the current in the electrochemical measurement (brown line in Fig. 5b) decreases when 4-AP electrogenerated passes through the filter, and simultaneously, absorbance value (blue line in Fig. 5b) increases because 4-AP is formed and it passes to the bottom side of the FS-SWCNT filter.

To determine the efficiency of this process, the molar absorption coefficients of 4-NP ($\varepsilon_{4\text{-}NP}$) and 4-AP ($\varepsilon_{4\text{-}AP}$) or difference value between them ($\Delta\varepsilon$) at 405 nm are needed. UV-vis absorption spectroelectrochemistry offers different possibilities to calculate these values. One of the simplest one consists of the estimation of the difference of the molar absorption coefficients

($\Delta\varepsilon = \varepsilon_{4\text{-}AP} - \varepsilon_{4\text{-}NP}$) when the reactant (4-NP) is completely electrolyzed into the product (4-AP) [53]. A chronoabsorptometry was performed to provoke an exhaustive electrolysis in the 4-NP solution sampled by the optical fibers in parallel arrangement. According to the Lambert-Beer's law (eq. 1), where A = 0.486 a.u., b = 0.056 cm and assuming that a 4-NP concentration of 5 × 10^{-4} M was completely reduced to 4-AP in the 100 μm closest to the electrode surface, the difference between the molar absorption coefficients of 4-NP and 4-AP at 405 nm is $\Delta\varepsilon$ = 17357 L mol^{-1} cm^{-1}. The efficiency of the reduction of 4-NP using FS-SWCNT electrochemical filters was calculated according eq. 3 at 405 nm. By the Lambert-Beer's law (eq. 1), and considering that $\Delta\varepsilon$ = 17357 L mol^{-1} cm^{-1} [65], b = 0.042 cm and C = 5 × 10^{-4} M, $A_{theoretical}$ is calculated (0.365 a.u). Taking into account that the mean maximum absorbance observed in Fig. 5b is 0.351 (obtained from the absorbance at 405 nm from 60 s onwards), the efficiency of this FS-SWCNT filter was calculated with eq. 2, obtaining a value of 96 %.

4. Conclusions

Combination of electrochemical FS-SWCNT filters and UV-vis absorption spectroelectrochemical techniques not only provokes the degradation of different compounds of wastewater but also allows the spectroelectrochemical monitoring of the whole process and the determination of the efficiency of the process. In this way, the development of new devices should facilitate this purpose. Quantitative information provided by UV-vis spectroelectrochemistry has demonstrated to be very useful in the determination of the efficiency of the electrochemical filtration process.

Acknowledgments

Financial support from Ministerio de Economía y Competitividad (CTQ2014-61914-EXP, CTQ2014-55583-R, TEC2017-85059-C3-2-R, CTQ2015-71955-REDT) and Junta de Castilla y León (BU033-U16) is gratefully acknowledged. D.I. thanks Ministerio de Economía y Competitividad for his postdoctoral fellowship (CTQ2014-61914-EXP). Jose Manuel Díez is acknowledged for his help in the fabrication of the electrodes (contract funded by the European Social Fund and the Youth Employment Initiative).

Appendix A. Supplementary data

Supplementary data associated with this article can be found in the online version.

AUTHOR INFORMATION

Corresponding Authors

e-mail: dibanez@ubu.es

e-mail: maheras@ubu.es

Tel: +34 947 25 88 17. Fax: +34 947 25 88 31

REFERENCES

[1] O. Abdelwahab, N.K. Amin, E.-S.Z. El-Ashtoukhy, Electrochemical removal of phenol from oil refinery wastewater, J. Hazard. Mater. 163 (2009) 711–716.

[2] Y. Deng, J.D. Englehardt, Electrochemical oxidation for landfill leachate treatment, Waste Manag. 27 (2007) 380–388.

[3] J.A. Rather, K. De Wael, Fullerene-C60 sensor for ultra-high sensitive detection of bisphenol-A and its treatment by green technology, Sensors Actuators B Chem. 176 (2013) 110–117.

[4] M. Gotsi, N. Kalogerakis, E. Psillakis, P. Samaras, D. Mantzavinos, Electrochemical oxidation of olive oil mill wastewaters, Water Res. 39 (2005) 4177–4187.

[5] A.G. Vlyssides, P.K. Karlis, N. Rori, A.A. Zorpas, Electrochemical treatment in relation

to pH of domestic wastewater using Ti / Pt electrodes, J. Hazard. Mater. B95 (2002) 215–226.

[6] M. Mavros, N.P. Xekoukoulotakis, D. Mantzavinos, E. Diamadopoulos, Complete treatment of olive pomace leachate by coagulation, activated-carbon adsorption and electrochemical oxidation, Water Res. 42 (2008) 2883–2888.

[7] Y. Esfandyari, Y. Mahdavi, M. Seyedsalehi, M. Hoseini, Degradation and biodegradability improvement of the olive mill wastewater by peroxi-electrocoagulation/electrooxidation- electroflotation process with bipolar aluminum electrodes, Environ. Sci. Pollut. Res. 22 (2015) 6288–6297.

[8] E. Chatzisymeon, N.P. Xekoukoulotakis, A. Coz, N. Kalogerakis, D. Mantzavinos, Electrochemical treatment of textile dyes and dyehouse effluents, J. Hazard. Mater. B137 (2006) 998–1007.

[9] M. Panizza, Electrochemical Oxidation as a Final Treatment of Synthetic Tannery Wastewater, Environ. Sci. Technol. 38 (2004) 5470–5475.

[10] F.C. Moreira, J. Soler, M.F. Alpendurada, R.A.R. Boaventura, E. Brillas, V.J.P. Vilar, Tertiary treatment of a municipal wastewater toward pharmaceuticals removal by chemical and electrochemical advanced oxidation processes, Water Res. 105 (2016) 251–263.

[11] M. Panizza, G. Cerisola, Direct And Mediated Anodic Oxidation of Organic Pollutants, Chem. Rev. 109 (2009) 6541–6569.

[12] I. Sirés, E. Brillas, Remediation of water pollution caused by pharmaceutical residues based on electrochemical separation and degradation technologies : A review, Environ. Int. 40 (2012) 212–229.

[13] N. Flores, I. Sirés, R.M. Rodríguez, F. Centellas, P.L. Cabot, J.A. Garrido, E. Brillas, Removal of 4-hydroxyphenylacetic acid from aqueous medium by electrochemical oxidation with a BDD anode: mineralization, kinetics and oxidation products, J. Electroanal. Chem. 793 (2017) 58–65.

[14] J.R. Steter, E. Brillas, I. Sirés, On the selection of the anode material for the electrochemical removal of methylparaben from different aqueous media, Electrochim. Acta. 222 (2016) 1464–1474.

[15] J.A. Rather, K. De Wael, C60-functionalized MWCNT based sensor for sensitive detection of endocrine disruptor vinclozolin in solubilized system and wastewater, Sensors Actuators B Chem. 171-172 (2012) 907–915.

[16] V. Vojinović, J.M.S. Cabral, L.P. Fonseca, Real-time bioprocess monitoring: Part I: In situ sensors, Sensors Actuators B Chem. 114 (2006) 1083–1091.

[17] Y.H. Kim, J.S. Park, H.I. Jung, An impedimetric biosensor for real-time monitoring of bacterial growth in a microbial fermentor, Sensors Actuators B Chem. 138 (2009) 270–277.

[18] H. Horry, T. Charrier, M.J. Durand, B. Vrignaud, P. Picart, P. Daniel, G. Thouand, Technological conception of an optical biosensor with a disposable card for use with bioluminescent bacteria, Sensors Actuators B Chem. 122 (2007) 527–534.

[19] K.D. Anders, G. Wehnert, O. Thordsen, T. Scheper, B. Rehr, H. Sahm, Biotechnological applications of fiber-optic sensing: multiple uses of a fiber-optic fluorimeter, Sensors Actuators B Chem. 11 (1993) 395–403.

[20] Z. Jin, Y. Su, Y. Duan, Improved optical pH sensor based on polyaniline, Sensors Actuators B Chem. 71 (2000) 118–122.

[21] A.R. Bakr, S. Rahaman, Electrochemical efficacy of a carboxylated multiwalled carbon nanotube filter for the removal of ibuprofen from aqueous solutions under acidic conditions, Chemosphere. 153 (2016) 508–520.

[22] G. Gao, C.D. Vecitis, Doped Carbon Nanotube Networks for Electrochemical Filtration of Aqueous Phenol: Electrolyte Precipitation and Phenol Polymerization, ACS Appl. Mater. Interfaces. 4 (2012) 1478–1489.

[23] X. Sun, J. Wu, Z. Chen, X. Su, B.J. Hinds, Fouling Characteristics and Electrochemical Recovery of Carbon Nanotube Membranes, Adv. Funct. Mater. 23 (2013) 1500–1506.

[24] J.I. Yang, J.U.N. Wang, J. Jia, Improvement of Electrochemical Wastewater Treatment through Mass Transfer in a Seepage Carbon Nanotube Electrode Reactor, Environ. Sci. Technol. 43 (2009) 3796–3802.

[25] G. Gao, Q. Zhang, Z. Hao, C.D. Vecitis, Carbon Nanotube Membrane Stack for Flow-through Sequential Regenerative Electro-Fenton, Environ. Sci. Technol. 49 (2015) 2375–2383.

[26] C.D. Vecitis, M. Elimelech, Electrochemical Carbon-Nanotube Filter Performance toward Virus Removal and Inactivation in the Presence of Natural Organic Matter, Environ. Sci. Technol. 46 (2012) 1556–1564.

[27] C.D. Vecitis, G. Gao, H. Liu, Electrochemical Carbon Nanotube Filter for Adsorption, Desorption, and Oxidation of Aqueous Dyes and Anions, J. Phys. Chem. B. 115 (2011) 3621–3629.

[28] M.H. Schnoor, C.D. Vecitis, Quantitative Examination of Aqueous Ferrocyanide Oxidation in a Carbon Nanotube Electrochemical Filter: Effects of Flow Rate, Ionic Strength, and Cathode Material, J. Phys. Chem. C. 117 (2013) 2855–2867.

[29] D. Ibañez, J. Garoz-Ruiz, A. Heras, A. Colina, Simultaneous UV–Visible Absorption and Raman Spectroelectrochemistry, Anal. Chem. 88 (2016) 8210–8217.

[30] D. Ibañez, E.C. Romero, A. Heras, A. Colina, Dynamic Raman Spectroelectrochemistry of Single Walled Carbon Nanotubes modified electrodes using a Langmuir-Schaefer method, Electrochim. Acta. 129 (2014) 171–176.

[31] D. Ibañez, A. Santidrian, A. Heras, M. Kalbáč, A. Colina, Study of adenine and guanine

oxidation mechanism by surface-enhanced Raman spectroelectrochemistry, J. Phys. Chem. C. 119 (2015) 8191–8198.

[32] K. Suganandam, P. Santhosh, M. Sankarasubramanian, A. Gopalan, T. Vasudevan, K.P. Lee, Fe3+ ion sensing characteristics of polydiphenylamine - electrochemical and spectroelectrochemical analysis, Sensors Actuators B Chem. 105 (2005) 223–231.

[33] N. González-Diéguez, A. Colina, J. López-Palacios, A. Heras, Spectroelectrochemistry at screen-printed electrodes: Determination of dopamine, Anal. Chem. 84 (2012) 9146–9153.

[34] C. Fernandez-Blanco, D. Ibañez, A. Colina, V. Ruiz, A. Heras, Spectroelectrochemical study of the electrosynthesis of Pt nanoparticles/poly(3,4-(ethylenedioxythiophene) composite, Electrochim. Acta. 145 (2014) 139–147.

[35] L. Kavan, L. Dunsch, Spectroelectrochemistry of Carbon Nanostructures, ChemPhysChem. 8 (2007) 974–998.

[36] J. Garoz-Ruiz, D. Izquierdo, A. Colina, S. Palmero, A. Heras, Optical fiber spectroelectrochemical device for detection of catechol at press-transferred single-walled carbon nanotubes electrodes., Anal. Bioanal. Chem. 405 (2013) 3593–3602.

[37] D. Ibañez, E. Vallés, E. Gómez, A. Colina, A. Heras, Janus electrochemistry: asymmetric functionalization in one step., ACS Appl. Mater. Interfaces. 9 (2017) 35404–35410.

[38] L. León, J.J. Maraver, J. Carbajo, J.D. Mozo, Simple and multi-configurational flow-cell detector for UV–vis spectroelectrochemical measurements in commercial instruments, Sensors Actuators B Chem. 186 (2013) 263–269.

[39] D. Izquierdo, V. Ferraresi-Curotto, A. Heras, R. Pis-Diez, A.C. Gonzalez-Baro, Bidimensional Spectroelectrochemistry: application of a new device in the study of a ovanillin-copper (II) complex, Electrochim. Acta. 245 (2017) 79–87.

[40] J. López-Palacios, A. Colina, A. Heras, V. Ruiz, L. Fuente, Bidimensional Spectroelectrochemistry, Anal. Chem. 73 (2001) 2883–2889.

[41] U.R. Lakshmi, V.C. Srivastava, I.D. Mall, D.H. Lataye, Rice husk ash as an effective adsorbent: Evaluation of adsorptive characteristics for Indigo Carmine dye, J. Environ. Manage. 90 (2009) 710–720.

[42] I. Othman, R.M. Mohamed, I.A. Ibrahim, M. Mokhtar, Synthesis and modification of ZSM-5 with manganese and lanthanum and their effects on decolorization of indigo carmine dye, Appl. Catal. A Gen. 299 (2006) 95–102.

[43] G. Rounaghi, R.M. Kakhki, H. Azizi-toupkanloo, Voltammetric determination of 4-nitrophenol using a modified carbon paste electrode based on a new synthetic crown ether/silver nanoparticles, Mater. Sci. Eng. C. 32 (2012) 172–177.

[44] D. Chaara, I. Pavlovic, F. Bruna, M.A. Ulibarri, K. Draoui, C. Barriga, Removal of nitrophenol pesticides from aqueous solutions by layered double hydroxides and their

calcined products., Appl. Clay Sci. 50 (2010) 292–298.

[45] Q. Chen, S. Mou, X. Hou, J.M. Riviello, Z. Ni, Determination of eight synthetic food colorants in drinks by high-performance ion chromatography, J. Chromatogr. A. 827 (1998) 73–81.

[46] US Environmental Protection Agency, Fed. Regist. 1979, 44, 233, Fed. Regist. 44 (1979) 23.

[47] US Environmental Protection Agency, Fed. Regist. 1989, 52, 131, Fed. Regist. 52 (1989) 131.

[48] S. Laha, K.P. Petrova, Biodegradation of 4-nitrophenol by indigenous microbial populations in Everglades soils, Biodegradation. 8 (1998) 349–356.

[49] M.J. Vaidya, S.M. Kulkarni, R. V Chaudhari, Synthesis of p-Aminophenol by Catalytic Hydrogenation of p-Nitrophenol, Org. Process Res. Dev. 7 (2003) 202–208.

[50] S. Chaliha, K.G. Bhattacharyya, P. Paul, Oxidation of 4-nitrophenol in water over Fe(III), Co(II), and Ni(II) impregnated MCM41 catalysts, J. Chem. Technol. Biotechnol. 83 (2008) 1353–1363.

[51] Rajeshwar, K., J.G. Ibanez, G.M. Swain, Electrochemistry and the environment, J. Appl. Electrochem. 24 (1994) 1077–1091.

[52] K. Nazari, N. Esmaeili, A. Mahmoudi, H. Rahimi, A.A. Moosavi-Movahedi, Peroxidative phenol removal from aqueous solutions using activated peroxidase biocatalyst, Enzyme Microb. Technol. 41 (2007) 226–233.

[53] J. Garoz-Ruiz, A. Heras, S. Palmero, A. Colina, Development of a Novel Bidimensional Spectroelectrochemistry Cell Using Transfer Single-Walled Carbon Nanotubes Films as Optically Transparent Electrodes., Anal. Chem. 87 (2015) 6233–6239.

[54] D. Ibañez, J. Garoz-Ruiz, D. Plana, A. Heras, D.J. Fermín, A. Colina, Spectroelectrochemistry at free-standing carbon nanotubes electrodes, Electrochim. Acta. 217 (2016) 262–268.

[55] D. Ibañez, M. Galindo, A. Colina, E. Valles, A. Heras, E. Gomez, Silver nanoparticles / free-standing carbon nanotube Janus membranes., Electrochim. Acta. 243 (2017) 349–356.

[56] R.D. Apostolova, O. V Kolomoets, M.O. Danilov, E.M. Shembel, Electrolytic Co, Ni-Bimetalsulfide Composites with Hydrophilizated Multi-Wall Carbon Nanotubes in a Prototype Lithium Accumulator, Surf. Eng. Appl. Electrochem. 50 (2014) 18–27.

[57] C. Chen, H. Su, S. Chuang, S. Yen, Y. Chen, Y. Lee, H. Chen, Hydrophilic modification of neural microelectrode arrays based on multi-walled carbon nanotubes, Nanotechnology. 21 (2010) 485501.

[58] Y. Li, C. Hung, C. Li, W. Chin, B. Wei, W. Hsu, A gas-phase hydrophilization of carbon

nanotubes by xenon excimer ultraviolet irradiation, J. Mater. Chem. 19 (2009) 6761–6765.

[59] S. Shanmugam, A. Gedanken, Generation of Hydrophilic , Bamboo-Shaped Multiwalled Carbon Nanotubes by Solid-State Pyrolysis and Its Electrochemical Studies, J. Phys. Chem. B. 110 (2006) 2037–2044.

[60] N. Wong, S. Kam, Z. Liu, H. Dai, Functionalization of Carbon Nanotubes via Cleavable Disulfide Bonds for Efficient Intracellular Delivery of siRNA and Potent Gene Silencing, J. Am. Chem. Soc. (2005) 12492–12493.

[61] M. Ujihara, T. Imae, A Review of Hydrophilization of Oxidized Nanocarbons, ACS Symp. Ser. 1215 (2015) 25–41.

[62] B. Shen, M. Olbrich-Stock, J. Posdorfer, R.N. Schindler, An Optical and Spectroelectrochemical Investigation of Indigo Carmine, Zeitschrift Für Phys. Chemie. 173 (1991) 251–255.

[63] P. Fanjul-Bolado, D. Hernández-Santos, P.J. Lamas-Ardisana, A. Martín-Pernía, A. Costa-García, Electrochemical characterization of screen-printed and conventional carbon paste electrodes, Electrochim. Acta. 53 (2008) 3635–3642.

[64] J. He, G. Ma, J. Chen, Y. Yao, Y. Wang, Electrochimica Acta Voltammetry and spectroelectrochemistry of solid indigo dispersed in carbon paste, Electrochim. Acta. 55 (2010) 4845–4850.

[65] Z.Y. Zhang, R.L. Vanetten, Pre-steady-state and steady-state kinetic-analysis of the low-molecular-weight phosphotyrosyl protein phosphatase from bovine heart, J. Biol. Chem. 266 (1991) 1516–1525.

Figures

Figure 1

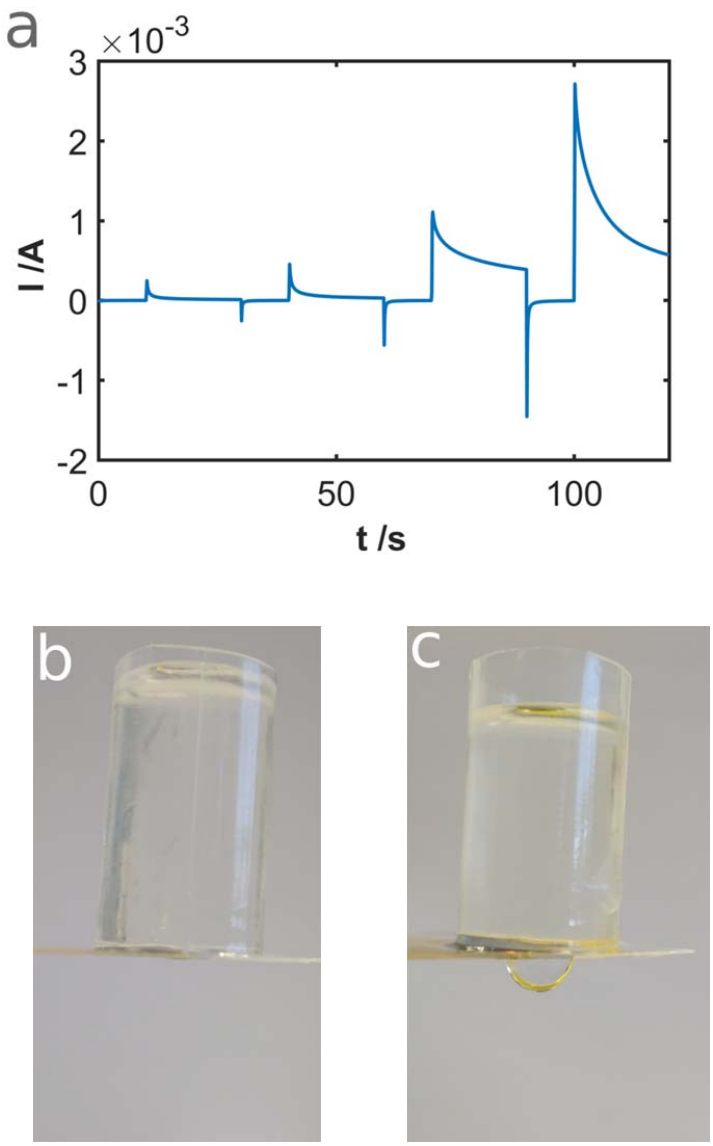

Fig. 1. (a) Chronoamperogram performed in 0.1 M NH_4PF_6 applying 0.00 V, 10 s; +1.20 V, 20 s; 0.00 V, 10 s; +1.40 V, 20 s; 0.00 V, 10 s; +1.60 V, 20 s; 0.00 V, 10 s and +1.80 V, 20 s. FS-SWCNT filter (b) before and (c) after the electrochemical functionalization.

Figure 2

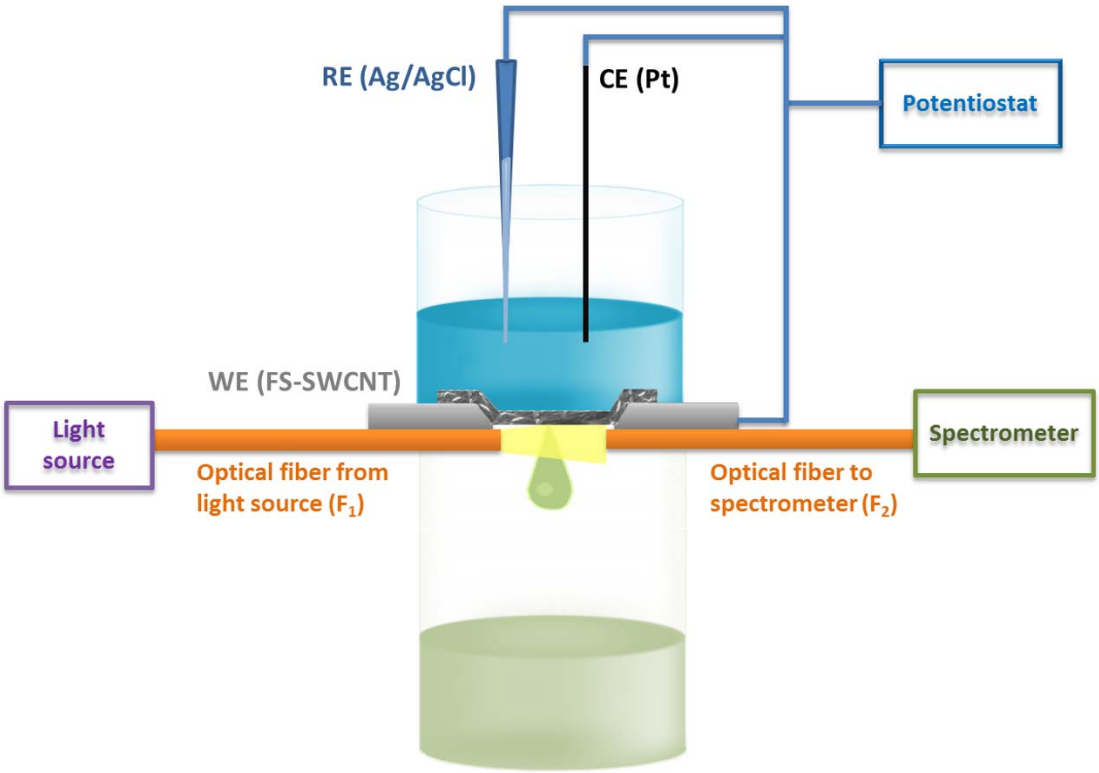

Fig. 2. Schematic view of the experimental setup, in which two optical fibers (F_1 and F_2) aligned and fixed on the bottom side of the filter provide the evolution of the UV-vis absorption signal in parallel configuration during the electrochemical experiment. The SEM image shows the area of the FS-SWCNT filter.

Figure 3

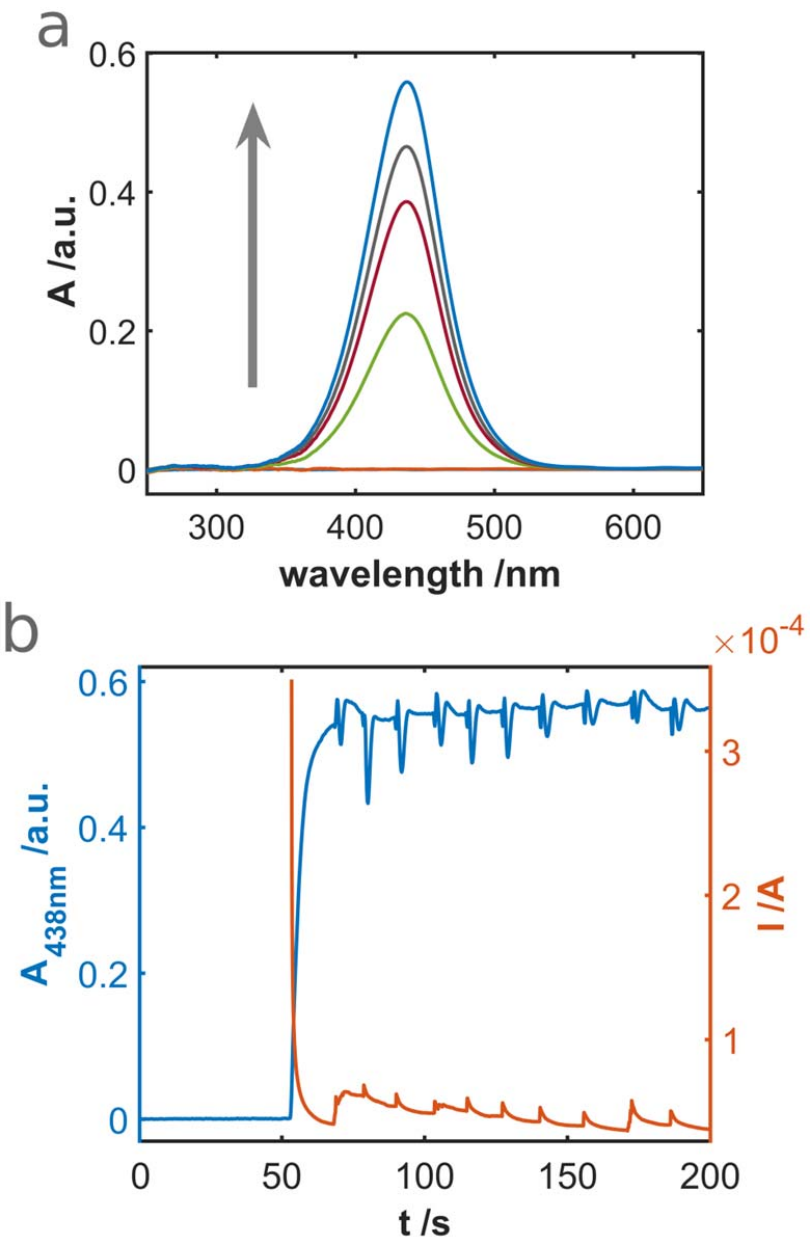

Fig. 3. (a) UV-vis absorption spectra recorded on the bottom side of the filter during the electrochemical oxidation from *o*-tol to *o*-tolidinium cation during the first 60 seconds of the chonoamperometric experiment. (b) Comparison of the evolution of the UV-vis absorbance at 438 nm (blue line) and the chronoamperogram (brown line) recorded during the electrochemical filtration. Integration time = 200 ms.

Figure 4

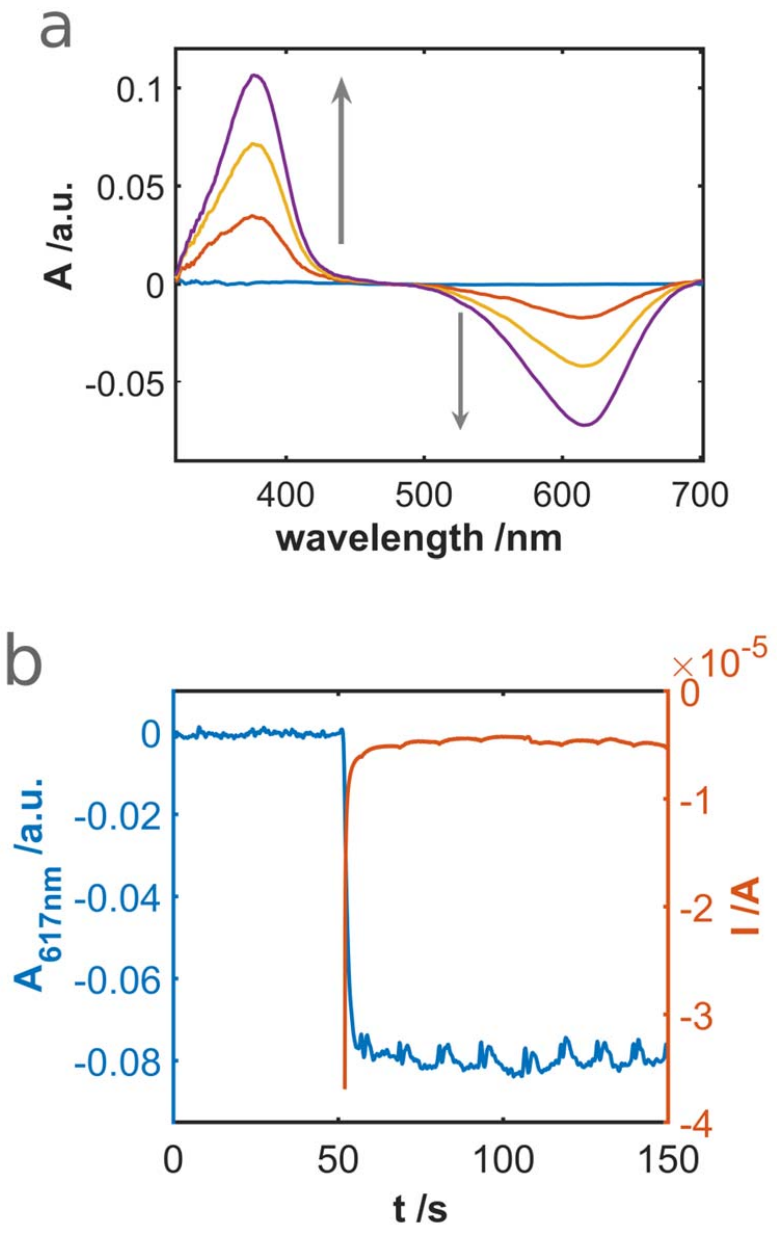

Fig. 4. (a) UV-vis absorption spectra recorded on the bottom side of the filter during the electrochemical reduction from IC to leuco-IC during the first 60 s of the chronoamperometric experiment. (b) Comparison of the evolution of the UV-vis absorbance at 617 nm (blue line) and

the chronoamperogram (brown line) recorded during the electrochemical filtration. Integration time = 200 ms.

Figure 5

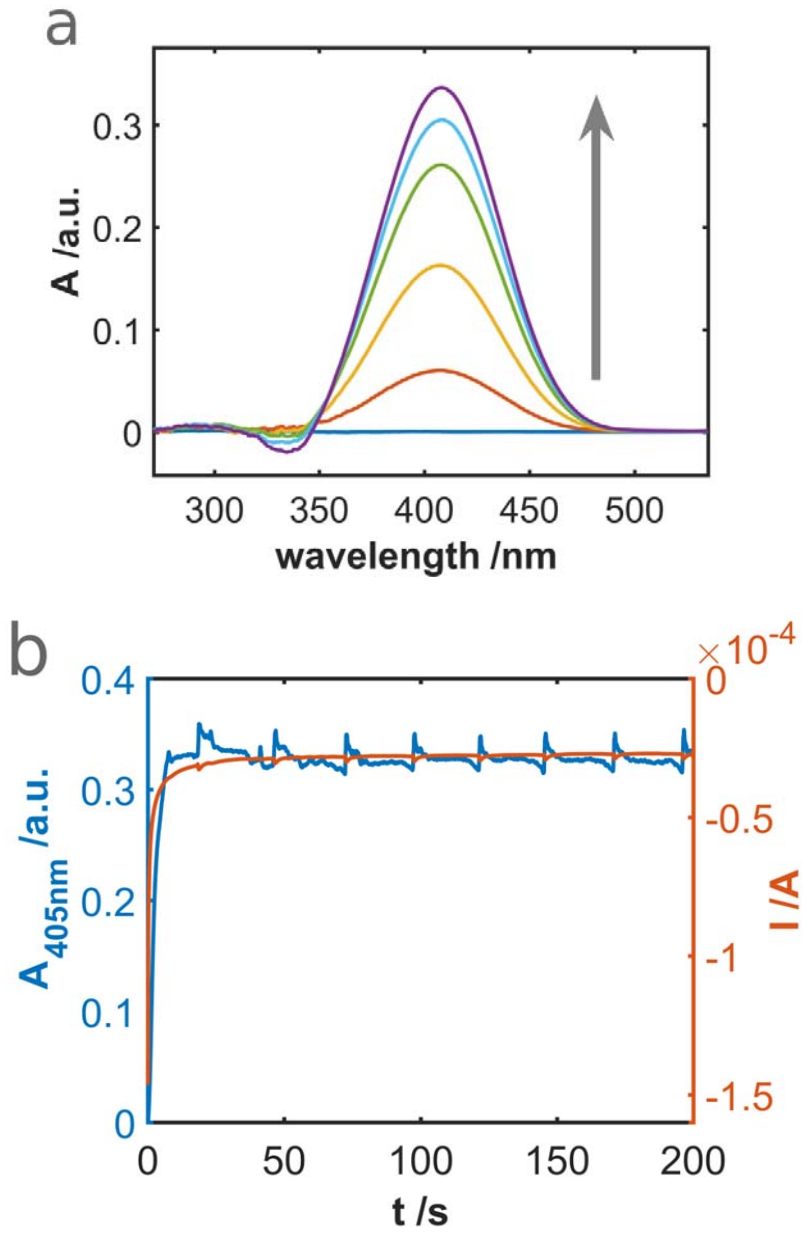

Fig. 5. (a) UV-vis absorption spectra recorded on the bottom side of the filter during the electrochemical reduction from 4-NP to 4-AP during the first 20 s of the chronoamperometric

experiment. (b) Comparison of the evolution of the UV-vis absorbance at 405 nm (blue line) and the chronoamperogram (brown line) recorded during the electrochemical filtration. Integration time = 50 ms.

Graphical abstract